6 The greenhouse effect and climate feedbacks

6.1 The greenhouse effect in Earth's current climate

6.1.1 Global energy balance

Recall the global energy balance (Figure 2.8) from Chapter 2. Here let us review it with an eye to creating a very simple globally averaged energy balance model that may then be used to understand the results from more complex climate models.

Recall also that the upgoing energy flux leaving the surface is actually *greater* than the net energy from the Sun arriving at the surface because the atmosphere traps most of the upgoing energy and re-radiates part of it back downward. This is the greenhouse effect, as seen in Earth's current climate, discussed in Chapter 2. We begin by examining this climatological greenhouse effect in more detail, before going on to examine impacts of changes to the greenhouse effect.

In Figure 6.1, essential aspects of the energy budget diagram are repeated using the format and notation that will be used for the global-average energy balance model. The energy input by solar energy of 342 W m^{-2} is immediately reduced by 31% (107 W m^{-2}) reflected back to space, and so a net solar flux of $S = 235$ W m^{-2} enters the climate system. About 20% (67 W m^{-2}) is absorbed in the atmosphere but the rest is absorbed at the surface for a net solar input at the surface of 168 W m^{-2}. Considering the surface energy budget, although the solar input is the driver of the system, the largest individual terms are the infrared radiation (IR) terms. The IR emitted upward from the surface is denoted $IR^{\uparrow}_{sfc}$ and the IR coming downward from the atmosphere is denoted $IR^{\downarrow}_{atm}$. Their values from Figure 2.8 are 390 W m^{-2} and 324 W m^{-2}, respectively, but they are left as symbols in Figure 6.1 because they are part of the solution that will be sought in the energy balance model. To a good approximation, all of $IR^{\downarrow}_{atm}$ is absorbed at the surface. A smaller additional upward energy flux from the surface is contributed by evaporation and sensible heat, for a total of 102 W m^{-2}.

At the top of the atmosphere, a total of 235 W m^{-2} of IR are emitted upward, as must occur if the system is in equilibrium, since the IR output must balance the net solar input into the system. Of the outgoing IR to space, only 40 W m^{-2} come directly from the Earth's surface. Of the $IR^{\uparrow}_{sfc}$ emitted upward, 90% (350 out of 390 W m^{-2}) is trapped in the atmosphere and only 10% exits directly to space. The rest of the upward IR toward space is emitted from the atmosphere itself, denoted $IR^{\uparrow}_{atm}$. Its value sets the characteristic emission temperature of the atmosphere.

https://doi.org/10.1017/CBO9780511780363.007 Published online by Cambridge University Press

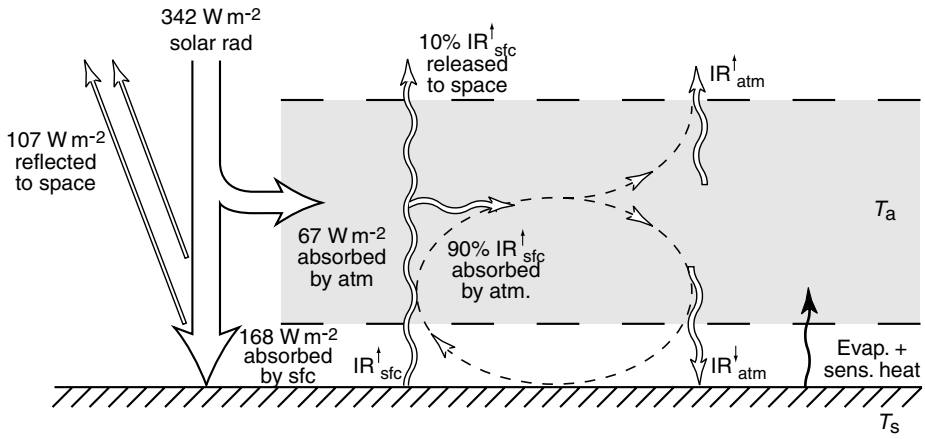

Fig. 6.1 A globally averaged energy balance model with a one-layer atmosphere. Solar radiation flux is shown on the left. Infrared fluxes are shown as wavy lines. Evaporation and sensible heat are indicated by a thin black arrow. The configuration shown approximates the global average energy budget. Simpler cases will be discussed.

6.1.2 A global-average energy balance model with a one-layer atmosphere

In the discussion of Figure 6.1 above, we have simply listed features from observations as they might be used in a globally averaged energy balance model. To make the model work, we need to consider how the fluxes depend on each other, and to include temperatures. There exist global-average energy balance models that include effects of vertical structure of temperature in the atmosphere, but here the simplest case is considered: that of a one-layer atmosphere model, which has a single atmospheric temperature, T_a. The surface has a different temperature, T_s. This model can already capture much of the basic physics of the greenhouse effect, since the atmosphere can absorb and emit differently than the surface.

Note that because the model treats only global averages, we do not have to deal with atmospheric or oceanic transports. The temperatures T_a and T_s represent globally averaged values, given the global-average solar input. Evaporation and sensible heat transfers from surface to the atmosphere can be included in this type of model, and we will include them in the discussion of processes, but for simplicity we can consider a case that neglects these. Thus IR is approximated as doing all the transfer from the surface to the atmosphere. This may seem a drastic approximation, but the IR terms are the largest individual terms in the surface budget, and evaporation and sensible heat increase with surface temperature in a manner qualitatively similar to IR. The Stefan–Boltzmann law for IR is simpler than the other dependences.

6.1.3 Infrared emissions from a layer

A fundamental property of emitted IR is essential to the greenhouse effect. For a parcel of gas of a single temperature, emissions are independent of direction. For the case of a layer, this means that upward emission is equal to downward emission. Because emissions

https://doi.org/10.1017/CBO9780511780363.007 Published online by Cambridge University Press

are associated with the random bouncing of molecules in the gas (as characterized by temperature), there is no reason for them to be any different for upward or downward emission. Thus for a layer of constant temperature

$$IR^{\uparrow}_{atm} = IR^{\downarrow}_{atm} \tag{6.1}$$

6.1.4 The greenhouse effect: example with a completely IR-absorbing atmosphere

Consider a simple case where the atmosphere is "black" in the IR, i.e. it simply absorbs all of the infrared that enters it. Let us begin with a case in which the atmosphere absorbs no visible, shown in Figure 6.2a. Balances of fluxes must occur at several levels, but the balance at the top is the most important, since this is the overall input and output from

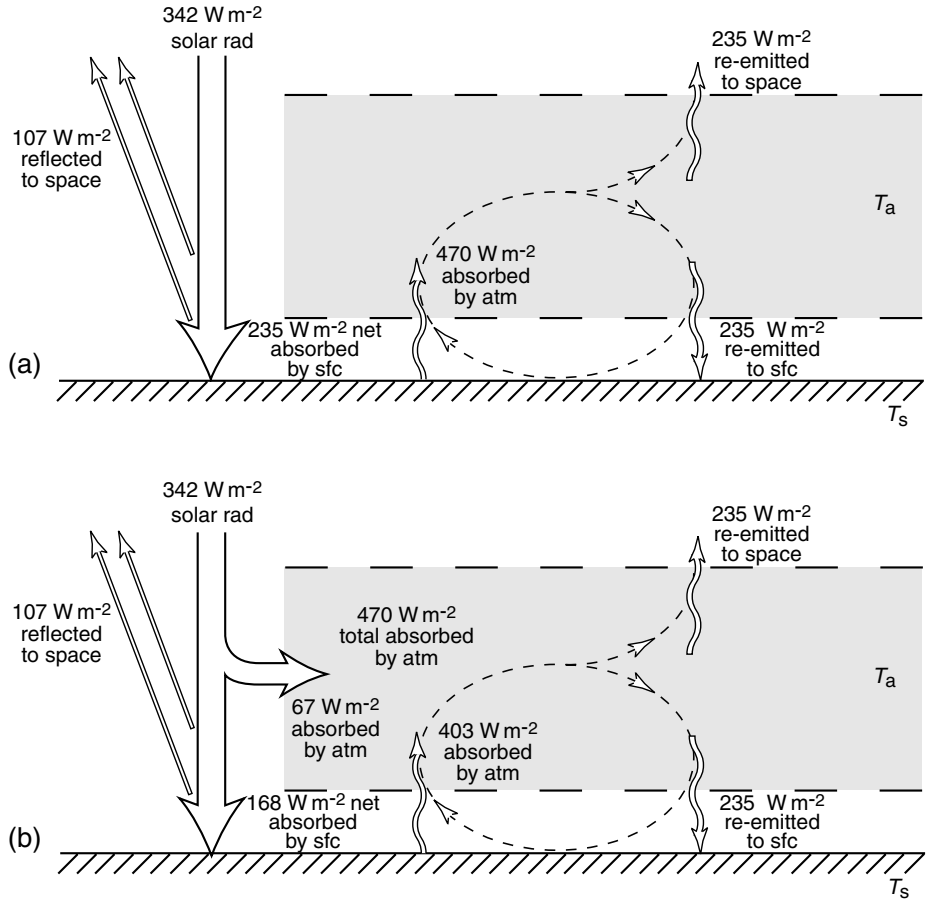

Fig. 6.2 Radiative fluxes for a simplified case where the atmosphere absorbs all infrared, as solved in the one-layer, global-average energy balance model for a given solar input. (a) The case where all solar goes through the atmosphere. (b) The case where a realistic portion of the solar radiation is absorbed in the atmosphere.

https://doi.org/10.1017/CBO9780511780363.007 Published online by Cambridge University Press

the Earth system. A net of 235 W m^{-2} of solar flux is going in, so 235 W m^{-2} of IR must leave. In this case, all of the IR emitted to space comes from the atmosphere (none from the surface) so the value of $IR^{\uparrow}_{atm}$ is 235 W m^{-2}. Using Eq. (6.1), the downward IR must also be 235 W m^{-2}. This is added to the solar flux arriving at the surface to give a total input to the surface of 470 W m^{-2}. The surface must balance this flux with $IR^{\uparrow}_{sfc}$ so this must therefore be 470 W m^{-2}. Clearly the surface must be warmer to emit 470 W m^{-2} than to emit 235 W m^{-2}, which would be the case if no atmosphere were present (if the albedo were kept the same). This is the greenhouse effect.

Note that we obtained this solution by working from the balance at the top of the atmosphere, and then considering the balance at the surface. It was obtained without actually solving for temperature, since relatively few terms enter the balances. In terms of sequence, if the solar input had been increased to the value shown from a lower value, the surface would heat up first, increasing $IR^{\uparrow}_{sfc}$ which would then heat the atmosphere. As the atmosphere began emitting to space and to the surface the surface temperature would heat up more owing to the greenhouse effect, thus heating the atmosphere more, and so on. This sequence would converge, with the temperature of the surface and atmosphere gradually approaching the balance shown. We have simply solved directly for the final equilibrium solution, without going through the time evolution.

Figure 6.2b shows a slightly more realistic case where the atmosphere absorbs 67 W m^{-2} of solar flux. The simplification of assuming that the atmosphere absorbs all of the IR emitted by the surface is still used in this case, so the balance at the top of the atmosphere that determines $IR^{\uparrow}_{atm}$ is exactly the same as the previous case. The atmosphere is absorbing more heat than in Figure 6.2a but $IR^{\uparrow}_{atm}$ is no different because it is set by the overall balance of the climate system, as seen at the top of the atmosphere. The downward IR flux is still set by Eq. (6.1). Because less solar radiation flux arrives at the ground than in the previous case (168 W m^{-2} instead of 235 W m^{-2}), the value of $IR^{\uparrow}_{sfc}$ is smaller (403 W m^{-2}), i.e. the surface is cooler.

6.1.5 The greenhouse effect in a one-layer atmosphere, global-average model

The atmosphere lets a portion of the upward IR from the surface through to space, which we neglected in the previous simple cases. In the global average energy budget, this was about 10%. This is important to the question of human changes to the greenhouse effect, because it is the fraction of IR absorbed that we are changing by adding greenhouse gases. In the one-layer model, we can include this effect, albeit crudely, by using a bulk absorptivity of the atmosphere for IR, $\epsilon_a = 0.90$. Of course, this is not exactly the same as the real atmosphere, because the atmosphere has temperature variation with height. Even if almost no IR were able to escape directly from the surface to space, adding greenhouse gases could increase surface temperature by changing the height from which upward IR primarily escapes to space, as opposed to being reabsorbed within the atmosphere. With higher greenhouse gases, the typical level within the upper troposphere from which IR is emitted to space shifts to higher heights, and the entire troposphere has to warm until these higher altitudes emit sufficient radiation to restore energy balance. The one-layer atmosphere omits these effects of vertical differences of temperature within the atmosphere,

https://doi.org/10.1017/CBO9780511780363.007 Published online by Cambridge University Press

but includes the difference between the atmospheric temperature and surface temperature. This approximation is sufficient to illustrate both the climatological greenhouse effect and changes to the greenhouse effect.

We now solve the energy balance model given in Figure 6.1 for a case where we neglect evaporation and sensible heat, since $IR^{\uparrow}_{sfc}$ is the dominant cooling term at the surface. Referring to the figure we find the following flux balances (in $\mathrm{W\,m^{-2}}$).

At the top of the atmosphere:

$$235 = (1 - \epsilon_a) IR^{\uparrow}_{sfc} + IR^{\uparrow}_{atm} \tag{6.2}$$

At the surface:

$$168 + IR^{\downarrow}_{atm} = IR^{\uparrow}_{sfc} \tag{6.3}$$

For a one-layer atmosphere:

$$IR^{\downarrow}_{atm} = IR^{\uparrow}_{atm} \tag{6.4}$$

So combining these, we find

$$IR^{\uparrow}_{sfc} = 403/(2 - \epsilon_a) \tag{6.5}$$

For $\epsilon_a = 0.90$, this gives $IR^{\uparrow}_{sfc} = 366\,\mathrm{W\,m^{-2}}$. This is smaller than the flux in the case of an atmosphere that was completely IR-absorbing. Changes to the greenhouse effect associated with changes in absorptivity involve only a few percent changes in the fluxes, but these can be significant to the global climate. Temperature changes implied by Eq. (6.5) when absorptivity changes will be examined in Figure 6.4, below.

Compared with the observed energy budget in Figure 2.8, the total flux up from the ground in observations ($492\,\mathrm{W\,m^{-2}}$, since evaporation and sensible heat also contribute in the real atmosphere) is greater than the upward surface flux in this simple one-layer model. This is because the downward IR flux at the bottom of the atmosphere is larger than the upward IR flux at the top, which gives an even larger greenhouse effect than in the simple model. In a more realistic model, Eq. (6.1) would apply to each layer and several layers would be needed to capture the fact that the atmosphere is warmer near the surface than high in the atmosphere. The warmer temperatures near the surface create the larger downward IR flux than in a one-layer model. Nonetheless, the one-layer model has a large climatological greenhouse effect as can be seen by comparing to the no-atmosphere case. And when studying changes to the greenhouse effect, principles can be understood in the one-layer model prior to turning to three-dimensional models for more accurate estimates.

6.1.6 Temperatures from the one-layer energy balance model

Once the fluxes have been calculated, we obtain temperatures from the energy balance model using the Stefan–Boltzmann law from Chapter 2:

$$\sigma T_s^4 = IR^{\uparrow}_{sfc} \tag{6.6}$$

$$\epsilon_a \sigma T_a^4 = IR^{\uparrow}_{atm} = IR^{\downarrow}_{atm} \tag{6.7}$$

https://doi.org/10.1017/CBO9780511780363.007 Published online by Cambridge University Press

where IR is in units of $\mathrm{W\,m^{-2}}$. For the one-layer atmosphere case above, this yields $T_s = 283.5\,\mathrm{K} = 10.4\,^{\circ}\mathrm{C}$. The atmospheric temperature is considerably colder, at $T_a = 249.7\,\mathrm{K} = -23.5\,^{\circ}\mathrm{C}$.

We can compare this to the case with no atmosphere (but reflecting the same fraction of incoming solar radiation), where

$$\sigma T_s^4 = 235$$

yields $T_s = 254\,\mathrm{K} = -19\,^{\circ}\mathrm{C}$. This is much colder than the average surface temperature of the Earth, which is about 15 °C or 288 K. It is also much colder than the temperature obtained from the energy balance model with the one-layer atmosphere (although this model does not give temperatures quite as warm as observed). The difference between the observed and the no-atmosphere case gives a measure of how much the greenhouse effect warms the planet under "normal" conditions: about 34 K. Thus the greenhouse effect is already operating very powerfully in our climate system, and is very beneficial at its current levels.

The atmospheric temperature from the one-layer atmosphere is close to the surface temperature in the no-atmosphere case, but slightly colder. In the case where the atmosphere is black in the IR, T_a is identical to the T_s from the no-atmosphere case. This is because the IR at the top of the atmosphere always has to balance the same incoming solar. If all emissions to space come from the surface, or all come from the atmosphere, the level that is doing the emitting has this temperature, which is termed the *emission temperature*. If most comes from the atmosphere, but part comes from the warmer surface, then the atmosphere is slightly colder than the emission temperature. In the observed atmosphere, this corresponds to infrared radiation escaping to space predominantly from the upper troposphere, where these temperatures typically occur.

6.2 Global warming I: example in the global-average energy balance model

6.2.1 Increases in the basic greenhouse effect

As discussed in Chapter 1, human activities are increasing the concentration of greenhouse gases – gases that significantly absorb infrared radiation – in the atmosphere. Let us first examine how this can cause warming without considering that clouds and other aspects of the climate system might also change. We will call this the "basic greenhouse effect" for ease of discussion later (terminology varies within the field). Figure 6.3 indicates schematically how these changes occur. The steps indicated in the figure are based on the one-layer atmospheric model, but hold qualitatively for more complex models. This is the same pathway as the greenhouse effect in climatology, simply increasing the effect. The atmospheric temperature in the one-layer model must be interpreted as a tropospheric temperature, since that is where the bulk of IR emissions originate. The stratospheric temperature actually cools when CO_2 is increased, as discussed in section 6.7.

https://doi.org/10.1017/CBO9780511780363.007 Published online by Cambridge University Press

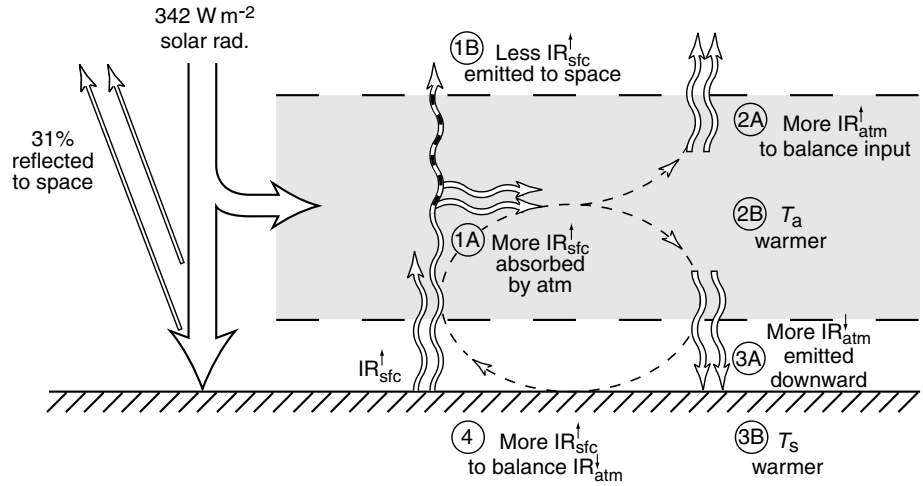

Fig. 6.3 Schematic of how increased absorption of infrared radiation by greenhouse gases leads to surface warming. Stages are shown in conceptual sequence from the point of view of energy balance requirements. (1) More upgoing IR from the surface is absorbed by the atmosphere and so does not escape directly to space. (2A) Since the input of solar energy is the same as always, while direct IR loss from the surface is decreased, more IR must be emitted from the atmosphere to achieve balance. This occurs by (2B) an increase in tropospheric temperature. A consequence of this is (3A) that more IR is emitted downward. To balance this increased input, there must be (4) increased IR upward from the surface, which occurs after (3B) surface temperature has increased sufficiently.

6.2.2 Climate feedback parameter in the one-layer global-average model

To calculate temperature increases in the one-layer global-average model when the greenhouse effect is increased, it is simple to increase ϵ_a to a new value, e.g. from 0.9 to 0.93, then repeat the calculation of total temperatures and subtract the temperatures that were calculated for the "normal" climatological value $\bar{\epsilon}_a$. This is a procedure similar to what is done in full climate models. When comparing models and effects of various processes, it is useful to define a *climate feedback parameter* α that gives the change in surface temperature per change in *radiative forcing*. This applies only approximately and for small changes. This parameter is illustrated here in the simpler model and given in a more general case in the following section with a related parameter, the climate sensitivity parameter. The term *forcing* generally refers to an external cause driving a response in a system. The radiative forcing here will be the change in infrared radiation in response to a specified change in greenhouse gas; this will then lead to a chain of feedbacks involving atmospheric and surface temperature and, as discussed in section 6.3, other parts of the climate system.

Figure 6.4 shows the dependence of surface temperature ϵ_a on in the one-layer global average model, using Eq. (6.5) and Eq. (6.6). Both equations are nonlinear – Eq. (6.5) depends inversely on $(2-\epsilon_a)$, and Eq. (6.6) yields a fourth root dependence – but for the range of interest, this curve is fit very well by a linear approximation matching the slope of

https://doi.org/10.1017/CBO9780511780363.007 Published online by Cambridge University Press

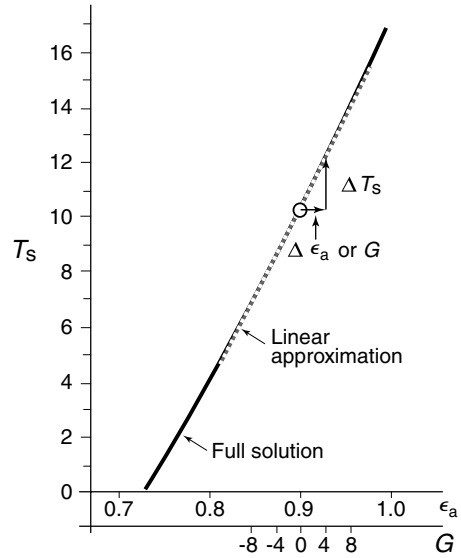

Fig. 6.4 Surface temperature (°C) as a function of absorptivity ϵ_a (unitless) in the one-layer global-average energy balance model. A linear approximation is shown as a dashed line. Using the solution at $\epsilon_a = 0.9$ as the reference climatology (open circle), the *x*-axis is also given as the top-of-the-atmosphere greenhouse radiative forcing G in W m^{-2}. Temperature change ΔT_s is also shown.

the nonlinear curve at the climatological value. This is an example of *linearization*, a useful and general approximation process that can also be done analytically on the equations.[1]

In a more complex model, the equivalent of ϵ_a is not a single number, since the absorptivity is calculated at many levels in the atmosphere and depends on concentrations of various greenhouse gases (GHG), among other things. In all cases, the radiative balance at the top of the atmosphere is key to the greenhouse effect, so by expressing the simple model in terms of changes in fluxes at the top of the atmosphere, we obtain an example that extends to other models. Consider adding an increase of greenhouse gas, corresponding in the simple model to an increase in absorptivity $\Delta\epsilon_a$, trapping more upgoing IR in the atmosphere. Before any temperature change occurs to compensate, there will be a deficit G in the outgoing IR causing an imbalance at the top of the atmosphere. The value of G, in W m^{-2}, is a good measure of the greenhouse radiative forcing (as a change from normal climatology). Note that G is independent of the particular gas that does the absorbing. In the case of the simple model, the total upward IR at the top of the atmosphere (from the right hand side of Eq. (6.2), using Eq. (6.3)) is

$$IR^{\uparrow}_{top} = (1 - \epsilon_a)\sigma T_s^4 + \epsilon_a(\sigma T_a^4) \tag{6.8}$$

The first term is the IR that gets through the atmosphere. The second term is $IR^{\uparrow}_{atm}$ which also depends on ϵ_a because emissivity equals absorptivity. Keeping the temperatures (temporarily) fixed at their climatological values, denoted $\bar{T}_s$ and $\bar{T}_a$, the reduction in outgoing IR due to a change in absorptivity $\Delta\epsilon_a$ is

https://doi.org/10.1017/CBO9780511780363.007 Published online by Cambridge University Press

$$G = \Delta\epsilon_a \sigma \bar{T}_s^4 - \Delta\epsilon_a \sigma \bar{T}_a^4 \tag{6.9}$$

The first term is the increased trapping of IR in the atmosphere, labelled 1B in Figure 6.3. This is the key term, causing the warming. The second term occurs because an increase in absorptivity implies an increase in emissivity. This term acts to reduce the effect of the first term, but is always smaller since the atmosphere is colder than the surface. Using the solution for $\epsilon_a = 0.90$ as the reference ("normal") climatology gives $G = 146.0\Delta\epsilon_a$. Computations from more complex models for doubled CO_2 give a value of about $4\,\mathrm{W\,m^{-2}}$ for G,[2] so using $\Delta\epsilon_a = 0.03$ gives a roughly comparable radiative forcing in the simple model.

After greenhouse gas increases cause the outgoing IR to decrease by G, temperature must warm to bring outgoing IR back into balance. For a linear approximation,[3] valid for sufficiently small ΔT_s as shown in Figure 6.4, ΔT_s is just proportional to G:

$$\alpha_T \Delta T_s = G \tag{6.10}$$

The quantity α_T is the *climate feedback parameter* (in units of $\mathrm{W\,m^{-2}\,K^{-1}}$) for this model. Here we are using α_T to denote the climate feedback parameter that arises only from changes in temperature (without any changes in water vapor, snow, ice clouds, etc.), and we will use α for a more general case in the next section. Note that ΔT_a can be obtained from ΔT_s using similar linearized balances. While G gives the changes in greenhouse gases as a change in radiative forcing, α summarizes the climate model feedbacks that determine the response ΔT_s. This value of α_T is proportional to the increase in outgoing IR at the top of the atmosphere per unit increase in surface temperature. Because T_a and T_s are linked by energy balance conditions, α_T takes into account also the effects of increases in atmospheric temperature.

The greenhouse effect is thus separated into two parts: (i) the additional absorption of IR in the atmosphere due to increased greenhouse gases. This is measured by the imbalance in outward IR, G, that occurs before temperature increases; (ii) the increase in outward IR to space due to warmer temperatures. This is a negative feedback which balances the heating effects of the forcing G. If the forcing were to disappear then this negative feedback would cause temperatures to go back toward normal.

The calculation of climate feedback parameters is subject to a number of caveats, and different variants appear in the literature. For example, different vertical structures of radiative heating change may have different effects on surface temperature even if they have the same change in the radiative fluxes at the top of the atmosphere. Nonetheless, the climate feedback parameter can still be used to illustrate the relative role of different feedbacks.

6.3 Climate feedbacks

The anthropogenic change due to the basic greenhouse effect acting by itself would be cause for only modest concern, since the amount of predicted warming would be fairly small on a global average. However, there are a number of climate feedbacks that modify changes due

https://doi.org/10.1017/CBO9780511780363.007 Published online by Cambridge University Press

to the basic greenhouse effect, and some of them may amplify it considerably. The main feedbacks are the *water vapor feedback*, associated with increases in water vapor, which itself is a greenhouse gas; the *snow/ice feedback*, due to decreases in snow and ice, causing global albedo to decrease (less solar radiation is reflected); and *cloud feedbacks*, due to changes in cloud cover, which affect the cloud contribution both to the greenhouse effect and to albedo.

The physics of these feedbacks will be discussed in more detail in the following subsections. First, let us use the framework from the global-average energy balance model to produce a simple notation for keeping track of the relative importance of feedbacks. Results from more complex models can then be diagnosed and discussed in this notation.

6.3.1 Climate feedback parameter

We wish to generalize the climate feedback parameter, so we can use the equation

$$\alpha \Delta T_s = G \tag{6.11}$$

to analyze the results of full climate models, where ΔT_s is the surface temperature change. If we can calculate a greenhouse forcing, G, then the ratio of the forcing to the temperature response can be defined as the climate feedback parameter α.

In the one-layer model of section 6.2, we had greenhouse gas forcing in terms of changes of the bulk absorptivity of the one-layer atmosphere, $\Delta\epsilon_a$. But for more complex models with many layers, the changes in absorption are not characterized by a single number. To calculate G from a complex model: (i) hold temperature, moisture, clouds, etc. *fixed* at their present climatological values; (ii) increase greenhouse gas concentrations; (iii) calculate the changes in outgoing IR flux at the top of the atmosphere (conventionally the top of the troposphere is used to avoid complications involving stratospheric response); (iv) take the global average. This gives a single number G (in $\mathrm{W\,m^{-2}}$) that characterizes the change in global-average radiative forcing of the system.[4]

Note that because temperatures are held fixed in this calculation, the greater amount of IR trapped by the increased greenhouse gases can produce the imbalance in top-of-atmosphere fluxes that gives G. When temperatures are allowed to change, they re-establish balance in the top-of-atmosphere fluxes, and α simply measures the size of temperature change that is needed to produce equilibrium.

In order to measure the effects of different feedbacks, one holds different parts of the climate system constant. For instance, to measure the negative feedback associated with increased IR loss to space as temperature increases, hold water vapor, ice, snow and clouds fixed at their climatological values, but allow temperature to vary. This defines the temperature contribution α_T to the climate feedback parameter. Contributions to α are approximately additive if the changes are small enough:

$$\alpha = \alpha_T + \alpha_{H_2O} + \alpha_{ice} + \alpha_{cloud} \tag{6.12}$$

where α_{H_2O} is the contribution of the water-vapor feedback, α_{ice} the contribution of the snow/ice feedback, α_{cloud} the net contribution of the cloud feedbacks. Formally, they are

https://doi.org/10.1017/CBO9780511780363.007 Published online by Cambridge University Press

defined by examining the change in the top-of-atmosphere energy balance with surface temperature

$$\alpha = \frac{\partial I R^{\uparrow}_{atm}}{\partial T_s} - \frac{\partial S}{\partial T_s} \tag{6.13}$$

where S is the net solar flux (global average) at the top of the atmosphere. Since incoming solar flux does not depend on Earth's surface temperature, the second term of α is really associated with changes in albedo, which change the amount of solar flux reflected back to space. In practice the diagnostics may be a bit more complicated.

Naturally, a simplified view like Eq. (6.11) cannot account for every aspect of climate change. In practice, the contributions of various feedbacks do not add as neatly as Eq. (6.12) would suggest, especially the cloud and snow/ice feedbacks. Other ambiguities include: different spatial distributions of flux or temperature may give different results even if the global average is the same; a change that is small in the global average may be large in some regions; and climate feedback parameter estimates by different approaches often do not agree exactly. It is simply a handy way of getting a feel for the behavior.

6.3.2 Contributions of climate feedbacks to global-average temperature response

Bearing these caveats in mind, Table 6.1 gives an estimate of the various contributions to the climate sensitivity parameter based on estimates from current climate models. The values in the table are a plausible example, taken from one study that uses a particular set of approximations. Other choices are sometimes used. For instance, this study used top-of-atmosphere fluxes for G and flux changes associated with each feedback. Other studies have used values at the tropopause, since the stratosphere actually cools, as discussed in section 6.7.1. This example illustrates how uncertainties in some feedback processes can give rise to considerable range of uncertainty in the computed warming. The overall range of uncertainty in ΔT_s in this study differs slightly from the range of equilibrium response of models in IPCC (1990) and IPCC (1992) to doubled CO_2, in which the range of 1.5 to 4.5 °C was listed. This range has remained similar in IPCC (1996) and IPCC (2001) and other recent estimates.

In Table 6.1, the first column shows the contribution of the feedback listed at the left, i.e. α_T, α_{H_2O}, α_{ice}, α_{cloud}, respectively, in Eq. (6.12). Physically, these correspond to the radiative heat loss to space per degree Celsius rise in surface temperature. The sign is thus positive for a negative feedback, i.e. an energy loss that opposes the warming, as is the case for the basic radiative feedback. The second shows the total climate feedback parameter including the feedback of that line and all feedbacks from previous lines. For instance, the value given beside ice/snow feedback includes the basic greenhouse effect (infrared cooling) and the water vapor feedback. The change in temperature in the third column is given by this value of α, with a value of the greenhouse radiative forcing of $G = 4.3\ \mathrm{W\ m^{-2}}$.

As may be seen from the implied temperature change, the size of the global average warming increases substantially when positive feedbacks are included. These tend to reduce the climate feedback parameter, so for the same forcing there is more warming. While a

https://doi.org/10.1017/CBO9780511780363.007 Published online by Cambridge University Press

Table 6.1 Example of the contributions of various feedbacks to the climate feedback parameter α and the surface temperature increase $\Delta T_s = G/\alpha$, using $G = 4.3\ \mathrm{W\,m^{-2}}$ for doubled CO_2.

Feedback	Radiative flux to space per degree increase in T_s ($\mathrm{W\,m^{-2}\,K^{-1}}$)	Cumulative climate feedback parameter, α ($\mathrm{W\,m^{-2}\,K^{-1}}$)	Cumulative change in equilibrium temperature ΔT_s(K)
Infrared cooling (Negative feedback)	3.7 to 4.4	3.7 to 4.4	1.0 to 1.2
Water vapor (Positive feedback)	–2.0 to –1.5	2.0 to 2.4	1.8 to 2.1
Sea ice/land snow (Positive feedback)	–0.3 to –0.1	1.7 to 2.3	1.9 to 2.5
Clouds (Positive to small)	–1.2 to –0.1	0.9 to 1.6	2.7 to 4.8

Note: While methods of estimating these feedbacks have limitations, the ranges of uncertainty typify current climate models, based on 12 models examined in Soden and Held (2006). Note that the range given for the cumulative climate feedback parameter is from the actual model values and is not the same as taking the sum of the lower and higher values of the first column. For instance, the model that has $\alpha_T = 3.7$ is not the same as the model that has $\alpha_{H_2O} = -2.0$, so the lowest value of 2.0 for $\alpha_T + \alpha_{H_2O}$ is larger than 3.7−2.0.[5]

1 °C warming (if it occurred slowly) might be acceptable, a 4 °C warming would have substantial consequences. And unfortunately, the feedbacks are in some of the most complex and difficult to model parts of the climate system. This results in the differences among the models that give the ranges shown, which can be viewed as rough estimates of the error bars on the representation of each process.

Thus, the climate feedbacks act to (i) increase the warming due to anthropogenic greenhouse gases; and (ii) increase the uncertainty in the estimate of this warming.

6.3.3 Climate sensitivity

Another common way of expressing the sensitivity of climate change to feedbacks is by the inverse of the climate feedback parameter

$$\lambda = \alpha^{-1} \tag{6.14}$$

This *climate sensitivity parameter*, λ, gives the surface temperature change per $\mathrm{W\,m^{-2}}$ change in the radiative forcing of the system. The climate sensitivity parameter is less used in recent literature, because the climate feedback parameter has advantages for comparing contributions of various feedbacks and when time dependence is included in the system.[6] Unfortunately, both of these parameters are based on approximations. They are sufficient to get a general idea of how climate feedbacks contribute to the size of the expected warming and to the error bars on climate model projections. As one asks more refined questions, however, the approach becomes awkward.

https://doi.org/10.1017/CBO9780511780363.007 Published online by Cambridge University Press

Table 6.2 The mean, standard deviation and range of doubled-CO_2 climate sensitivity (global-averaged surface temperature response) from models included in recent IPCC reports. Range refers to highest and lowest values from among all models.[7]

Publication	No. of models	Mean	Standard deviation	Range
IPCC (1996)	17	3.8 °C	0.8 °C	1.9 to 5.2 °C
IPCC (2001)	15	3.5 °C	0.9 °C	2.0 to 5.1 °C
IPCC (2007)	18	3.2 °C	0.7 °C	2.1 to 4.4 °C

A different approach is to define a standardized experiment that is relevant to future warming but straightforward to conduct with many models. This can then be used as a benchmark for comparing models. The standard experiment is to double CO_2 in the model and then run the simulation long enough that the model comes to a new equilibrium climate state, as described in more detail in section 6.8.2. The change in the long-term average then defines the model *doubled-CO_2 response*. The global-average surface temperature response ΔT_{2x} (subscript $2x$ is often used for 2 times CO_2) is then used as a measure of climate sensitivity. It is referred to as the *doubled-CO_2 climate sensitivity* or just the *climate sensitivity*.

Rather than attempt to separate different feedbacks as is done in Table 6.1, another approach aims to summarize the overall climate response. The last line of the ΔT_s column in Table 6.1 is an example of the doubled-CO_2 climate sensitivity. The range is illustrative of the spread among different climate models but actually underestimates the full range. Table 7 gives the spread in sensitivity among recent climate models in two ways: as a mean and standard deviation among the set of models, and as the range from lowest sensitivity to highest sensitivity. Note that the uncertainty, as measured by the spread among models, has not reduced much with time although the models have considerably improved representations of many processes.

6.4 The water vapor feedback

In rough terms, the physics of the water vapor feedback is very simple. Warmer air can hold more water vapor. In a warmer climate, the troposphere will have the potential to hold larger concentrations of water vapor. Water vapor is an effective greenhouse gas (the most important greenhouse gas in the climatological greenhouse effect), and thus it can add greatly to the initial warming if it increases. Figure 6.5 shows this process.

Because this is a positive feedback, in which warming due to the water vapor feedback further increases water vapor, one might worry that this effect might compound itself indefinitely. Indeed it might, if the increase in water vapor were enough to overcome the negative feedback that is always present in the system: that due to the increased IR loss with increased temperature. On Earth this does not happen, as can be seen from Table 6.1,

https://doi.org/10.1017/CBO9780511780363.007 Published online by Cambridge University Press

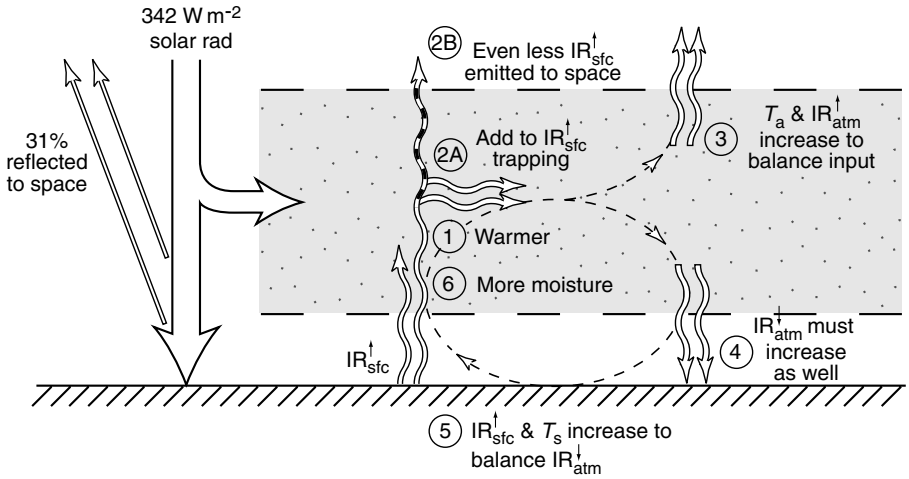

Fig. 6.5 Schematic of water vapor feedback in the greenhouse effect. (1) The initial warming by the basic greenhouse effect allows the atmosphere to hold more water vapor. (2) This increases IR trapping and reduces the IR lost directly to space from the surface, just as in the basic greenhouse effect. (3) The atmospheric temperature must warm until increased upward IR from the atmosphere compensates for the reduction in IR escaping from the surface to space. (4) Since atmospheric temperature has increased, downward IR increases also, resulting in (5) increased surface temperature until increased upward IR from the surface can balance the extra input from the atmosphere. (6) The warming due to the water vapor feedback itself increases water vapor.

since the water vapor impact on outward IR is only half that of the feedback due to temperature. If the positive feedback contributed more warming per temperature rise than the blackbody effect contributes cooling, one could have a "runaway greenhouse effect" in which temperatures continue to increase until some other regime of behavior is reached. It is sometimes speculated that such an effect might have occurred on Venus sometime in that planet's history.

The water vapor feedback is not without complications. Figure 6.6 shows in more detail the step between the fact that a warmer atmosphere can hold more water and the assumption that it actually does contain more water. The arrow marked Warmer, an example of the range of typical vapor pressure values after warming, assumes that relative humidity stays in a comparable range to current climate. While the shift in the mean vapor pressure is small compared with the range of variation, this case indeed implies a mean increase in water vapor. And competition among evaporation, transport and condensation indeed tends to keep the relative humidity more constant than the humidity itself, at least in the lower troposphere where contact with the moist lower boundary, combined with vertical mixing by convection, tends to keep parcels from becoming very dry. A parcel with low relative humidity reaching the surface causes evaporation to increase, and a parcel with high relative humidity that is perturbed significantly upward tends to lose water by condensation and precipitation.

In the upper troposphere, on the other hand, much of the water vapor is supplied by lateral mixing at very large scales. This carries water from the tropics, where frequent

https://doi.org/10.1017/CBO9780511780363.007 Published online by Cambridge University Press

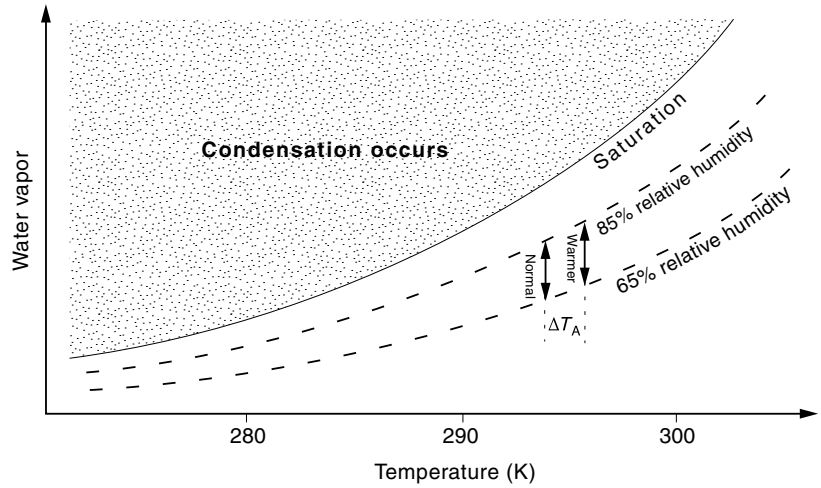

Fig. 6.6 Water vapor (as measured by vapor pressure) versus temperature, schematizing how water vapor might increase in global warming. The solid curve is the saturation value of vapor pressure as a function of temperature. Condensation would occur in an air parcel with initial vapor and temperature values to the upper left of this curve. An air parcel might have any combination of temperature and vapor corresponding to a point below this curve; the fraction of the saturation value at a given temperature is the relative humidity. Dashed curves show vapor pressure values as a function of temperature for 85% and 65% relative humidity. Atmospheric values of water vapor quite commonly fall between these lines. For a particular latitude and height, the arrow marked "Normal" indicates a typical range of water vapor pressures in the normal climate. After global warming, if the *relative* humidity remains in the same range, the arrow marked "Warmer" shows the range of vapor pressure in the warm climate.

deep convection tends to moisten the upper troposphere, to higher latitudes, where deep convection is more rare. This process largely conserves water during the trajectory from the tropics, and it is not clear that fixed relative humidity is a good approximation to its net effects. Recalling from section 6.1.6 that IR emission to space occurs more effectively from the upper troposphere, this upper tropospheric contribution to the water vapor greenhouse effect is at least as important as the lower troposphere, even though the latter has more water.

Until recently, it was difficult to get good data with global coverage for upper tropospheric water vapor. Standard weather balloon soundings often had inaccuracies, and enormous gaps in spatial coverage. Recently satellite sensors have been designed to estimate upper tropospheric water vapor. This is helping to determine how accurately climate models can simulate this quantity, and should begin to narrow the range of uncertainty on this feedback.

6.5 Snow/ice feedback

Given an initial warming by the basic greenhouse effect, snow and ice cover will tend to be reduced. Since both are highly reflective surfaces, they normally are responsible for a significant amount of reflected sunlight at high latitudes. Thus more sunlight is absorbed

https://doi.org/10.1017/CBO9780511780363.007 Published online by Cambridge University Press

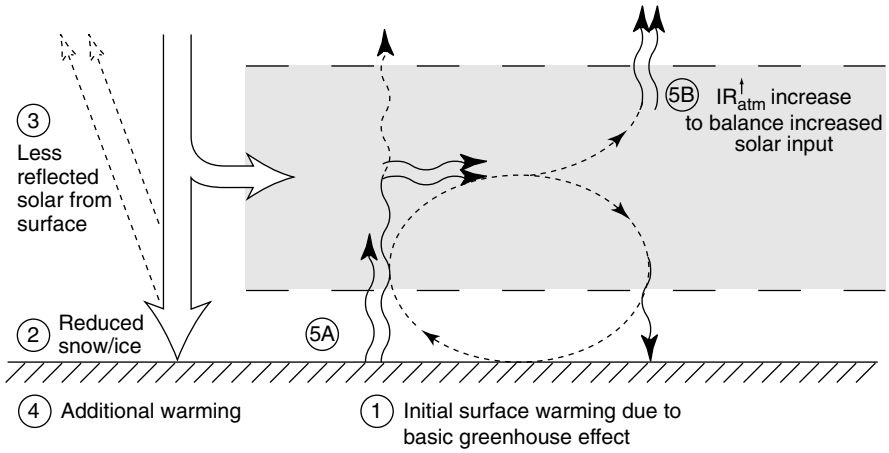

Fig. 6.7 Schematic of the snow/ice feedback in the global energy balance. Beginning with the initial warming at the surface caused by the basic greenhouse effect, the reduction (2) of snow and ice leads to (3) less reflected solar, i.e. greater net solar input into the climate system. This leads to (4) additional warming of the surface until (5) increased upward heat flux from the surface and warming of the atmosphere give enough increase in upward IR to space to balance the additional solar input.

at the Earth's surface in the warmer climate. This warms the climate still further. This is schematized in Figure 6.7, from the point of view of the global energy balance.

Of course, the snow/ice feedback, also known as the surface-albedo feedback, is felt most strongly in fairly high latitudes, and has a seasonal dependence, since it occurs at the boundary of the snow/ice cover. In Table 6.1, it appears to be only a modest effect in the global average, but this is an average of a large effect at higher latitudes with no effect in the tropics. Thus the snow/ice feedback can be quite important to the impact of global warming. Although the basic principle of this feedback is simple, it has recently been realized that there can be considerable interaction with cloud effects, since both reflect sunlight, and since snow cover can affect the local conditions under which clouds are forming.

6.6 Cloud feedbacks

Cloud feedbacks are challenging to represent in climate models for three reasons:

(i) Clouds are small-scale motions compared with the grid size of climate models. Their average effects at the grid size must be parameterized on large-scale motions.
(ii) Clouds have opposing effects in infrared and solar contributions to the energy budget.
(iii) Several types of cloud properties can affect radiative processes: these include cloud fraction, cloud top height, cloud depth, and cloud water and ice content. Different cloud types will thus have different feedbacks. Cloud amount is usually measured as *cloud fraction*, i.e. for a given area, such as a 200 km square grid box, the fraction that

https://doi.org/10.1017/CBO9780511780363.007 Published online by Cambridge University Press

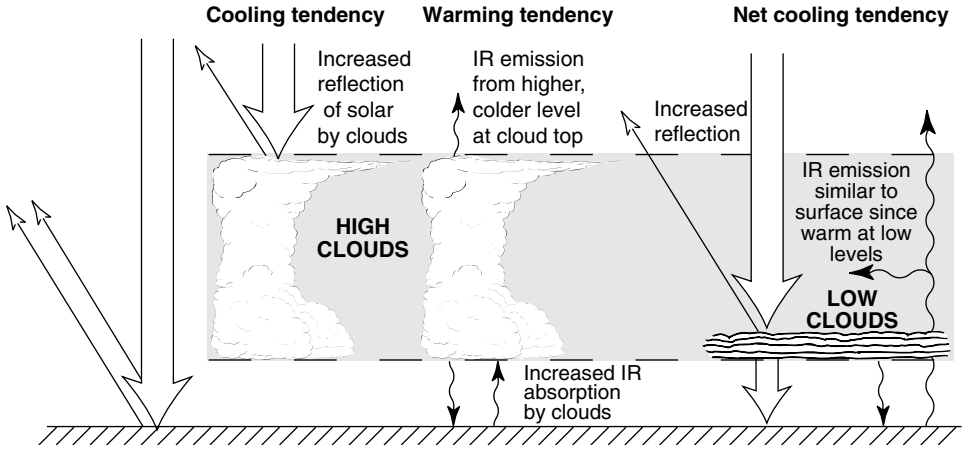

Fig. 6.8 Schematic of effects of cloud amount in the global energy balance. The feedback depends on whether the cloud fraction increases for a given cloud type. This figure shows cases of increased deep cloud fraction and low cloud fraction. Solar effects are shown on the left cloud, and infrared effects on the right hand cloud. If cloud fraction increases in a warmer climate, solar effects give a negative feedback, while IR effects give a positive feedback. For deep clouds these effects are similar in magnitude. For low clouds, the IR effects are smaller because the cloud top temperature is closer to surface temperature, so IR emitted from the cloud top is not changed as strongly.

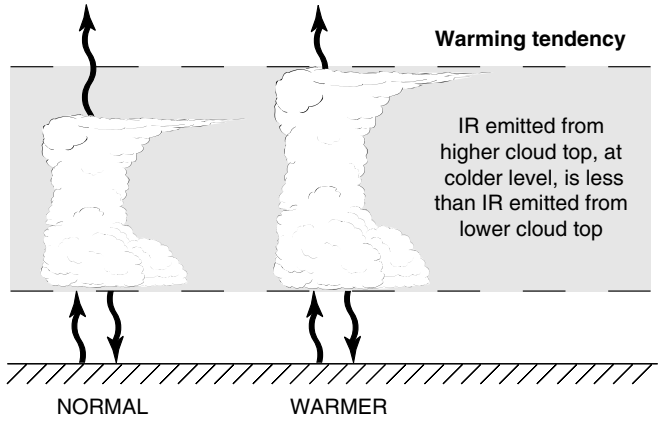

Fig. 6.9 Schematic of cloud top feedback. Cloud top tends to reach higher (and thus colder) levels because low-level moisture and temperature are increased. IR emissions from colder cloud top are thus decreased (a positive feedback).

is covered by cloud of a given type. Among several cloud feedbacks currently being studied, the schematics in Figure 6.8 and Figure 6.9 illustrate two of the better understood ones. Note that the cloud fraction feedback is really two opposing feedbacks, one involving reflection of solar and the other emission of IR from cloud top. The case illustrated for deep clouds in Figure 6.8 – in which there is considerable cancellation between these two effects – tends to apply also to other clouds with high tops, such as cirrus.

https://doi.org/10.1017/CBO9780511780363.007 Published online by Cambridge University Press

In Figure 6.8, the feedback depends on fraction of cloudy versus clear areas. Whether or not the fractional area covered by a certain type of cloud increases or decreases in a warmer climate depends on many aspects of the circulation. On a global average there will tend to be slightly more precipitation. However, increased intensity of convection in one region could actually lead to a reduction in some types of clouds in a neighboring region. Considering for example the case of increased cloud fraction, there are still two competing effects. More solar radiation will be reflected, since clouds have high albedo. This will likely tend to cool the climate, so if the warmer climate has more clouds, this is a negative feedback. On the other hand, the additional cloud region will trap more upgoing IR from the surface. It emits IR, but from cloud top, where the temperature is much colder, hence less IR will be emitted. This has a warming effect. For high clouds, the two effects tend to cancel fairly strongly (although not exactly). For clouds with tops at low levels, such as stratus clouds, the IR emission is from a temperature that is less cold (and more similar to the surface temperature), so the difference in IR emitted upward in cloudy or clear sky is smaller. Thus the solar effect dominates for low clouds.

Another feedback, the *cloud top feedback*, is illustrated in Figure 6.9. Even if the cloud fraction were to remain constant, the average height of the cloud top might change for certain cloud types in a warmer climate. If the surface layer were warmer and moister, but the temperature at upper levels did not warm enough to compensate, rising cloud parcels would tend to go slightly higher before reaching their level of stability, as discussed in Chapter 3. In climate model simulations, this tends to happen for deep convection. If the cloud top is higher, it occurs at a cooler temperature since the temperature drops with height. The IR emitted from cloud top is thus smaller than in the normal climate. This implies a warming tendency, i.e. a positive feedback.

There are a number of other postulated cloud feedbacks, including possible increases in cirrus cloud fraction, or increases in the reflectivity of clouds due to increased water content. These are subjects of current research. So far, it does not appear that new information on cloud feedbacks is greatly altering the best estimate of climate sensitivity, but rather is helping to refine the range of uncertainty.

6.7 Other feedbacks in the physical climate system

6.7.1 Stratospheric cooling

While the surface and troposphere warm when greenhouse gases are increased, the stratosphere tends to cool. This is because when greenhouse gases increase in the stratosphere, the absorbtion and emission of IR both increase. However, the balance of warming versus cooling effects differs from that in the troposphere. Consider adding a stratospheric layer of temperature T_{strat} onto the global average energy balance model. A simple stratospheric layer heat balance is

$$2\epsilon_{strat}\sigma T_{strat}^4 = Q_{ozone} + \epsilon_{strat} I R_{trop}^{\uparrow} \tag{6.15}$$

https://doi.org/10.1017/CBO9780511780363.007 Published online by Cambridge University Press

The first term is cooling by IR emission from the stratosphere (both upward and downward, yielding the factor of 2). This is balanced by heating by ozone absorption of solar radiation Q_{ozone} plus absorption of IR coming up from the troposphere and surface $IR^{\uparrow}_{trop}$. After the surface and troposphere regain energy balance with the new levels of greenhouse gases, $IR^{\uparrow}_{trop}$ is approximately the same. Increased greenhouse gases in the stratosphere cause ϵ_{strat} to increase on both sides of the equation. However, $IR^{\uparrow}_{trop}$ is not twice as large as the normal climatological value of ϵT^4_{strat}, so the cooling on the left hand side would initially increase more until T_{strat} can adjust to compensate. This implies that T_{strat} must decrease to maintain balance.

6.7.2 Lapse rate feedback

When the surface warms, the lower troposphere warms a roughly similar amount. The warming tends to increase slightly with height, so the upper troposphere experiences a larger warming. This implies that the lapse rate is decreasing slightly, hence the name of this feedback. The slightly increased warming in the upper troposphere causes more IR emission to space from the upper troposphere than if the warming were constant with height. This is part of the negative feedback by temperature, opposing the warming, given by α_T in Table 6.1. It can be useful to split α_T into a part α_0 that assumes the warming is constant with height and a lapse rate feedback contribution α_{LR}, such that $\alpha_T = \alpha_0 + \alpha_{LR}$. The reason for this is that the lapse rate change can vary from model to model, and usually changes considerably as a function of latitude since the lapse rate is set by deep convection in most of the tropics, while at high latitudes it is determined by balances involving atmospheric transports at upper levels versus boundary layer effects at low levels. Breaking out the lapse rate feedback separately helps gauge the uncertainty in these processes. In Table 6.1, α_0 is about 3.2 W m^{-2}, with only small changes among models. The lapse rate feedback accounts for most of the uncertainty in α_T. However, there tends to be substantial compensation between uncertaintly in the lapse rate feedback and the water vapor feedback. A model with slightly larger warming in the upper troposphere (larger negative feedback) tends to hold more water vapor in the upper troposphere (larger positive feedback). This is why the range in the cumulative feedback parameter $(\alpha_T + \alpha_{H_2O})$ in Table 6.1 is smaller than one might guess from the individual ranges of α_T and α_{H_2O}.

6.8 Climate response time in transient climate change

6.8.1 Transient climate change versus equilibrium response experiments

Experiments where the climate forcing is increased initially and then held fixed are termed equilibrium response experiments because the climate model is run until it reaches a statistical equilibrium state with a warmer climate. This is useful for comparing climate models and obtaining a view of the features of warmer climate in a controlled situation where the spatial pattern of the warming is not continually changing. The model can be run long

https://doi.org/10.1017/CBO9780511780363.007 Published online by Cambridge University Press

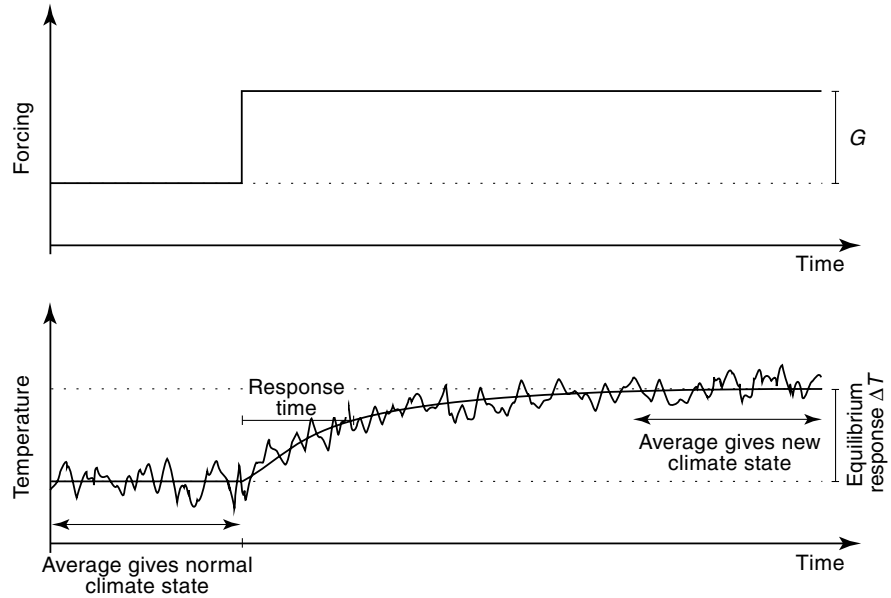

Fig. 6.10 Schematic of an equilibrium response experiment. The upper panel indicates the time dependence of the climate forcing. This could be the concentration of greenhouse gases, but is more often measured as the radiative forcing G resulting from an increase in concentration. The lower panel shows global average temperature response. The smooth curve gives the response of an energy balance model with a simple ocean. The jagged curve gives a time series more like a full climate model with weather and interannual variations (for clarity, interdecadal variations are less here than in a full climate system). The time axis covers a few hundred years. To accurately assess climate change, averaging periods longer than those shown would in fact be required.

enough in the warmer climate state that reliable statistics can be produced by averaging over a longer time period. Figure 6.10 shows a schematic example of such an experiment. The climate forcing, in this case by greenhouse gases, is increased suddenly at a certain time. The initial radiative imbalance at the top of the atmosphere is a good measure of the climate forcing. This would be equivalent to the forcing G discussed in the simple energy balance model of section 6.2. A typical experiment is to double CO_2 at the initial time, since this is a forcing that we are likely to reach in the middle of the twenty-first century. The initial radiative disequilibrium for this case is about $4\,W\,m^{-2}$. Such doubled-CO_2 experiments are used as benchmark of the climate sensitivity of models. A model that has a larger equilibrium warming in such an experiment is said to have a larger climate sensitivity, as discussed in section 6.3.3.

After greenhouse forcing is increased, there is a time period during which the model global average temperature warms toward the new equilibrium. The typical time scale of this warming is termed the response time of the climate system. It tends to be on the order of decades for global average surface temperature, owing to the heat capacity of the upper ocean. The climate system equilibrates with more than one response time, so a complete picture would first have the upper ocean approach near-equilibrium on a time scale of decades, then continue to adjust by smaller amounts over longer periods as the deep ocean

https://doi.org/10.1017/CBO9780511780363.007 Published online by Cambridge University Press

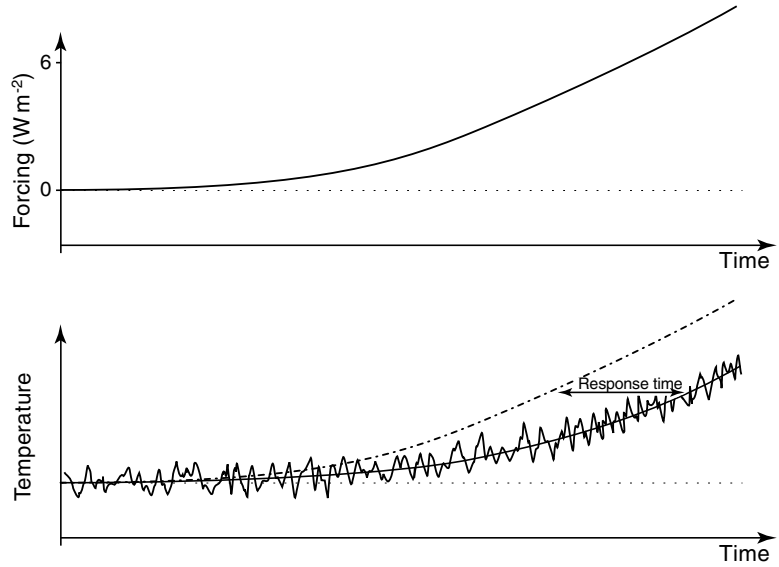

Fig. 6.11 Schematic of a greenhouse warming scenario with a time-dependent forcing, i.e. a transient response experiment. The upper panel shows the forcing as a function of time, typical of a 1% per year increase in carbon dioxide. In the lower panel, the smooth curve shows the temperature response for a simple energy balance model and the jagged curve shows a typical time series for a full climate model. The dashed curve gives the response of the system in the idealized case where the atmosphere is in equilibrium with the forcing.

equilibrates. In Figure 6.10 averaging periods to define the climate before the increase in forcing and after equilibration are indicated. Owing to natural interdecadal variability in the climate system, decades are required to establish accurate climate statistics. For quantities with high variance, such as regional precipitation, longer averaging periods would ideally be used.

In reality, greenhouse gas concentrations are increasing smoothly as a function of time, and experiments using such time-dependent forcing are termed *transient response experiments*. Because the forcing continues to change during the run, the climate response never quite catches up to the new forcing. During the time it takes the system to respond to previous increases in forcing, the forcing has increased even further. This may be seen in Figure 6.11, where for comparison an idealized case where the system is in equilibrium at every moment is included (dashed curve). This may be thought of as a case where the ocean has small heat capacity, although in practice it would be computed differently, since reducing ocean heat capacity would affect the seasonal cycle. In practice, it would have to be computed by running the model to equilibrium at each new value of the forcing, which would be very costly in a full climate model but is straightforward in an energy balance model.

In such a transient response experiment, there is no statistically steady averaging period that can be used to define a new climate. In order to separate natural variability from the forced increase, the method is to perform several climate model runs with the same forcing, but slightly different atmospheric and oceanic initial conditions. The set of such runs is known as an *ensemble*. Weather variations and interannual climate variations such as

https://doi.org/10.1017/CBO9780511780363.007 Published online by Cambridge University Press

El Niño will evolve differently in each run, whereas the response to the forcing will occur the same way. When many such runs are averaged, this *ensemble average* gives the response to the forcing. Unfortunately, it is computationally expensive, so only a few such runs are typically done in practice.

The climate model experiments we will see in Chapter 7 are affected by the heat capacity of the ocean in the manner schematized in Figure 6.11. The time-dependent response of the climate system lags behind the forcing and thus the warming is substantially less at each time than if the response had come to equilibrium with the GHG concentrations of that time. A consequence of this is that if society waits until a substantial warming has been detected before taking any action, the eventual warming will be larger. This is illustrated in Figure 6.12 using a case in which greenhouse forcing increases initially as in Figure 6.11, but then is suddenly held constant, corresponding to society suddenly realizing the problem is serious and stopping all emissions on the spot. There is still substantial warming until equilibrium with the forcing is achieved. This additional warming is termed the *additional warming commitment*, because at a given time we have committed the planet to warm this additional amount further than it has already warmed, even if we cease greenhouse gas emissions. A consequence of this additional warming commitment is that if one waits until

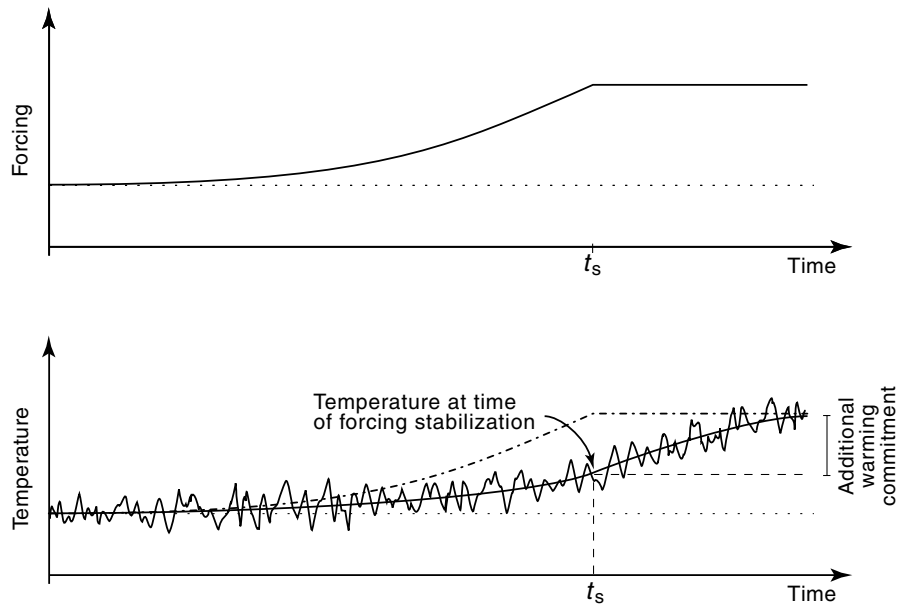

Fig. 6.12 A transient response experiment as in Figure 6.11, but where greenhouse gas emissions are suddenly stopped at time t_s, so the forcing stabilizes (upper panel). In the lower panel, the dashed curve shows the temperature response if the climate system were in equilibrium with the forcing. Since the ocean slows the response of the climate system, the actual temperature response (solid curve) lags behind the forcing. Thus the temperature continues to rise even after the emissions are stopped. The transient response eventually reaches equilibrium, but not until many decades later. The difference between the temperature at a given time (here shown for time t_s) and the equilibrium value (dashed curve) is termed the additional warming commitment.

https://doi.org/10.1017/CBO9780511780363.007 Published online by Cambridge University Press

it is clear that global warming is going to be large, there are substantial risks. This factor adds to the need to plan ahead in considering strategies to reduce emissions.

To provide a more detailed view of the spatial structure of warming in equilibrium versus the warming at a particular time, we turn to a classic climate model experiment that corresponds conceptually to the case shown in Figure 6.12. An experiment in which CO_2 increases at 1% per year (similar to observed increases over recent decades) will be examined. The warming that occurs around 70 years into the run, at the time when CO_2 has doubled, will be compared to the equilibrium response in a doubled-CO_2, experiment. This corresponds to the temperature the model would eventually reach if the CO_2 increase were stopped at t_s = 70 years and held constant until the model reached equilibrium.

6.8.2 A doubled-CO_2 equilibrium response experiment

As noted above, doubled-CO_2 experiments are used for understanding the general features of the response to increased gases, for comparing climate models, and as a measure of climate sensitivity. Unless special circumstances happen (such as a drastic collapse of the thermohaline circulation), the equilibrium response is independent of the history of the forcing and initial climate conditions, so such an experiment could be conducted, for instance, as shown in either Figure 6.10 or Figure 6.12 and the long-term results would be the same.

Figure 6.13a shows results for the equilibrated climate change for surface air temperature, with one of the climate models that was important in much of the early work on global warming. This model had a climate sensitivity on the high side of the range for current climate models but the main results continue to hold. A number of features of the spatial pattern of global warming may be seen in the equilibrium response in Figure 6.13a which will be discussed in more detail for more realistic, time-dependent scenarios. The surface warming is widespread over the globe in this model with a global-average equilibrium warming of about 4.5 °C. Warming occurs also throughout the troposphere. The warming is greater over midlatitudes than in the tropics and is even greater in polar regions, as will be discussed further in Chapter 7.

6.8.3 The role of the oceans in slowing warming

Turning to the time-dependent run from the same model, Figure 6.13b and c illustrate the spatial dependence of the ocean effect in slowing warming. In Figure 6.13b, the surface air temperature is shown for a 20-year average centered on the time at which CO_2 has doubled in a 1% per year CO_2 increase experiment. While the GHG radiative forcing in Figure 6.13b is the same as in Figure 6.13a, the heat capacity of the upper ocean (above the thermocline) has reduced the warming everywhere relative to the equilibrium response. Furthermore, in certain regions the warming is reduced even more effectively. This occurs in the North Atlantic and in the Southern Ocean near Antarctica where the thermohaline overturning carries heat down into the deep ocean. The warming is still largest in the high latitude regions of the northern hemisphere, but the oceanic effects have greatly delayed the

https://doi.org/10.1017/CBO9780511780363.007 Published online by Cambridge University Press

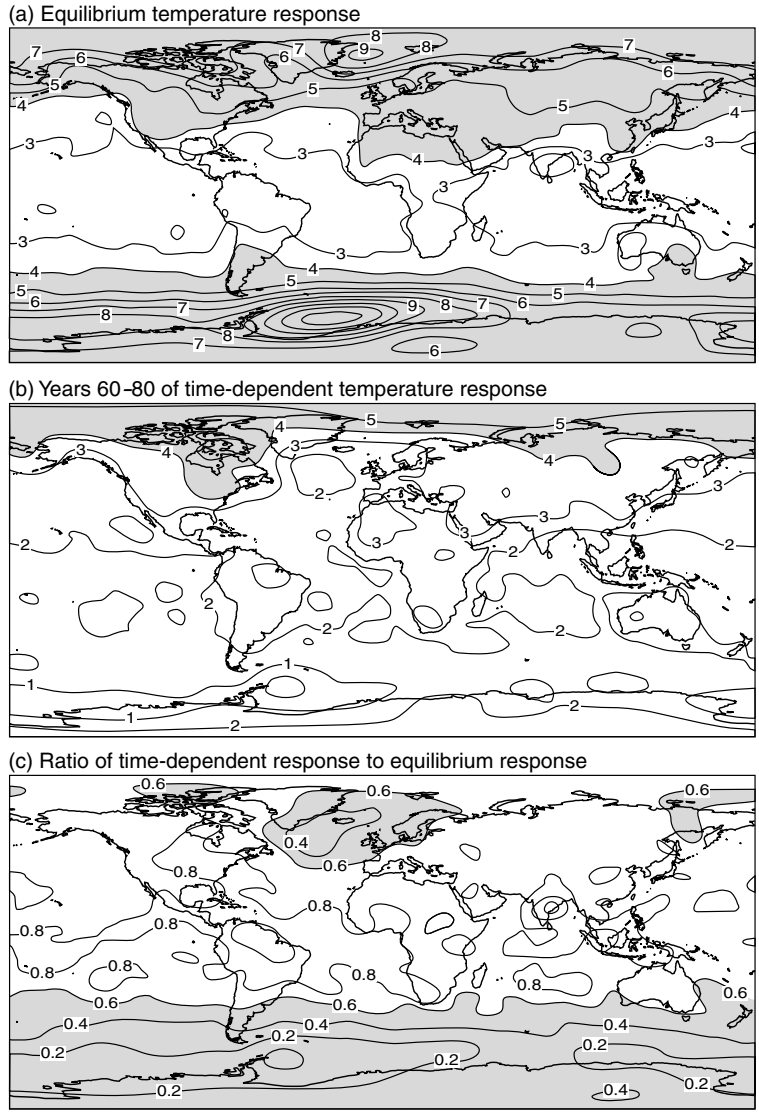

Fig. 6.13 Annual average surface air temperature response from an earlier version of the Geophysical Fluid Dynamics Laboratory climate model comparing equilibrium response to time-dependent response. (a) Equilibrium response for a doubled CO_2 experiment shown as difference from a control run. Contour interval 1 °C. (b) Coupled ocean–atmosphere model response to a 1% per year CO_2 increase shown at approximately the time that CO_2 has doubled in the model (averaged from years 60–80 of the model run) shown as a difference from a similarly averaged period from a control run. Contours as in (a). (c) Ratio of the time-dependent response in (b) to the equilibrium response in (a). Shading in (c) indicates regions where the time-dependent response is less than 60% of the equilibrium response. After Manabe *et al*. (1991).

https://doi.org/10.1017/CBO9780511780363.007 Published online by Cambridge University Press

warming in Antarctic regions. Northern hemisphere continents tend to have warmed more than neighboring oceanic regions.

The difference between Figure 6.13a and Figure 6.13b gives the global warming commitment at the time of doubled CO_2, as estimated by this model. If concentrations were held fixed at the time represented by 6.13b, the Earth would gradually warm to the situation in Figure 6.13a as the oceans approached equilibrium with the GHG forcing. Another view of the slowing of the warming by the oceans is shown in Figure 6.13c which displays the ratio of the two cases. In the time-dependent experiment at year 70, much of the globe has warmed by about 60% to 80% of the equilibrium value. The shaded area indicates the large regions that have warmed by less than 60% of what they will eventually attain, some by as little at 20%. These ratios may be taken as indicative of how the warming we might see in the middle of this century would compare to the long-term warming if GHG concentrations were capped at that time.

6.8.4 Climate sensitivity in transient climate change

For additional insight into the role of the oceans in slowing the warming, we take the simple globally averaged energy balance model of Eq. (6.11), and extend it to include the heat storage in an ocean surface layer of a specified depth, H. Heat storage in the atmosphere is negligible on these time scales, so any imbalance in the energy balance at the top of the atmosphere is associated with the ocean heat storage. The heat capacity per unit area of the layer is $C = \rho c_w H$, where ρ and c_w are the density and heat capacity per unit mass of sea water, as in the surface layer discussed in section 3.3.1. This simple climate model, including a heat storage term proportional to the rate of change of surface layer temperature, becomes

$$C\frac{\partial \Delta T_s}{\partial t} + \alpha \Delta T_s = G \tag{6.16}$$

Figure 6.14 shows a simple example that helps to understand the effects of different climate sensitivity in different climate models in the context of transient climate change. The greenhouse forcing G is a simplified case where the radiative forcing begins to go up linearly in 1970, at a rate that roughly mimics experiments in climate models. If the heat capacity of the ocean were negligible, the first term could be dropped and the equilibrium value of the global average temperature change would be

$$\Delta T_s = \frac{G}{\alpha} \tag{6.17}$$

and would go up linearly with G. These equilibrium curves are shown as dashed lines in Figure 6.14.

The ocean response time introduces a lag given by $\tau = C/\alpha$ (to see this, substitute the solution $\Delta T_s = g(t-\tau)/\alpha$ into Eq. (6.16), using $G = gt$). This lag gives the response time indicated in Figure 6.10 or Figure 6.11. After an initial adjustment period the temperature increases at the same rate as the equilibrium case, but the actual temperature lags the equilibrium solution by this response time. Different values of the climate feedback parameter α thus have two effects. If α is smaller (i.e. climate sensitivity is higher), then the

https://doi.org/10.1017/CBO9780511780363.007 Published online by Cambridge University Press

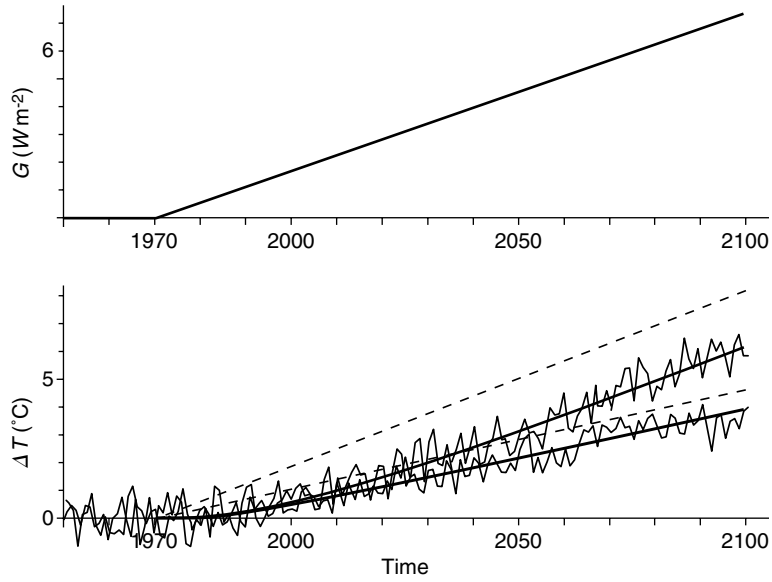

Fig. 6.14 Schematic of transient climate response to the forcing shown in the upper panel by climate models of different climate sensitivities. In the lower panel, the upper solid curve gives the global-average surface temperature response for a climate feedback parameter typical of the more sensitive climate models in IPCC (2001), while the lower curve would be typical of the less sensitive models. The dashed lines show the temperatures for each case that would occur if the ocean did not act to delay the warming. Because the response time is longer in the high sensitivity case, the curves initially look similar even though the long term response is very different. Wiggly lines indicate the natural climate variability that would occur about the simplified response curves.[8]

temperature increases more quickly in the long term. However, smaller α also implies a longer adjustment time, so it takes longer for this increase to begin. Not only does the heat capacity of the ocean slow the warming initially, it slows it more for the higher sensitivity case. Thus in the early stages after the forcing starts to increase, the curves for both the low sensitivity model and the high sensitivity model look very similar, even though the long-term outcome will be very different. Another way to see this is directly from Eq. (6.16). At early times, the change in temperature is still small, so the $\alpha \Delta T_s$, term does not contribute much to the balance. Rather, the ocean heat storage is the main balance for the radiative forcing initially. This delays the warming by an amount of time that depends on the heat capacity of the ocean (which enhances the storage term) versus α (which affects the size of the $\alpha \Delta T_s$ term).

This effect has considerable practical implications. We would like to know which model, the higher sensitivity model or the lower sensitivity model, better represents the actual climate system. We might imagine that we could wait, increasing our observational time series, until we could distinguish that one case was clearly a better fit. Because both remain similar for a long period, the disadvantage of this strategy is that a substantial warming would have already begun and an additional warming commitment would have been incurred. This is exacerbated by the presence of natural variability in the climate system which makes the

https://doi.org/10.1017/CBO9780511780363.007 Published online by Cambridge University Press

two curves hard to distinguish in the early stages of the warming. We will see in Chapter 7 how these principles apply to runs with full climate models.

Notes

1 Linearization can be applied more generally, for multiple variables, in combination with Taylor series. Recall that for a smooth function F of variables X and Y $\Delta F(X,Y) \approx \frac{\partial F}{\partial X}\Delta X + \frac{\partial F}{\partial Y}\Delta Y +$ (higher order terms), where changes are defined as $\Delta X = (X - \bar{X})$, and derivatives are evaluated at X, Y. Higher order terms means quadratic and higher powers in the changes, which can be neglected if the changes are small. For the case of the one-layer energy balance model, the equations can be linearized when a small temperature increase ΔT_s is to be calculated. For instance, the change in upward surface flux is approximately

$$\Delta IR^{\uparrow}_{sfc} \cong \left(\frac{\partial \sigma T_s^4}{\partial T_s}\right)\Delta T_s = 4\sigma \bar{T}_s^3 \Delta T_s \tag{6.18}$$

The first step applies when the changes are sufficiently small and the second step is simply differentiating Eq. (6.5). Overbars indicate climatological terms.

2 In IPCC (1996) and IPCC (1990), $G = 4.4\,\mathrm{W\,m^{-2}}$ was used. Myhre *et al*. (1998) suggest that, accounting for stratospheric adjustment and some solar absorption by CO_2, a more suitable number would be $3.7\,\mathrm{W\,m^{-2}}$.

3 While Figure 6.4 shows a numerical linearization, for this simple model it can also be done analytically. When only small changes are considered, it is possible to separate the changes in the fluxes due directly to changes in absorptivity $\Delta\epsilon_a$ from those due to changes in temperature. The change in IR at the top of the atmosphere is

$$\Delta IR_{top} \approx -G + (1 - \bar{\epsilon}_a)\Delta\left(\sigma T_S^4\right) + \bar{\epsilon}_a \Delta\left(\sigma T_a^4\right).$$

The balance is approximate because we have dropped a term $\Delta\epsilon_a \Delta IR^{\uparrow}_{sfc}$ that involves changes multiplying changes ("quadratic" in the changes). This is small since the changes are only a few percent of the climatological terms. Dropping the quadratic terms is one step in the linearization. One then applies a proceedure similar to Eq. (6.18) to obtain a linear relation.

4 Some authors use the global average flux at the bottom of the atmosphere. This can give self-consistent notation as well, although some of what is treated as feedback here is treated as forcing in that case.

5 The Soden and Held (2006) study from which Table 6.1 is adapted uses a method described in Held and Soden (2000) in which changes in temperature, water vapor and surface albedo (primarily sea ice and snow) from various models have their radiative effects evaluated individually using a single radiative scheme. Cloud feedbacks are estimated as a residual from other contributions and the overall value of α_T. Climate changes are from 10-year averages shortly after CO_2 doubling, and they use a $4.3\,\mathrm{W\,m^{-2}}$ nominal forcing for all models to evaluate α from the temperature change. For comparison, IPCC (1990) gave $\alpha_T = 3.3\,\mathrm{W\,m^{-2}\,K^{-1}}$ and $\alpha_{H_2O} = -1.2\,\mathrm{W\,m^{-2}\,K^{-1}}$, owing to different choices of how to evaluate these. The range of cloud feedback in the climate models examined in Cess *et al*. (1989, 1996), excluding outliers was roughly -0.8 to 0.6 (i.e. contained uncertainty even in sign), while for surface albedo feedback it was similar to Table 6.1. Overall, however, the relative contributions of the various feedbacks are fairly consistent as noted in the survey by Colman (2004).

6 Notation in the field varies. Sometimes α is used for the climate sensitivity and λ for the climate feedback parameter.

https://doi.org/10.1017/CBO9780511780363.007 Published online by Cambridge University Press

7 Based on IPCC (2001) Table 9.4 for the first two rows, and IPCC (2007) section 8.6.2.2 (see also section 10.5.2 and Box 10.2) for the last row.

8 The curves in Figure 6.14 use climate feedback parameter values of $\alpha = 0.9$ and 1.9 for the high and low sensitivity case, respectively. This would roughly correspond to the CSM1.0 and CSIRO models cited in IPCC (2001) section 9.3 and Appendix 9A. These are relatively high and low sensitivity models, although not the most extreme cases. The slope of the radiative forcing is $0.043\,\mathrm{W\,m^{-2}\,yr^{-1}}$, roughly mimicking the B2 scenario with moderate GHG emissions of Figure 7.2. The response times use an ocean mixed layer depth of 200 m, to crudely represent upper ocean adjustment for the layer above the thermocline, giving roughly 30 and 14 years for high and low sensitivity, respectively.

https://doi.org/10.1017/CBO9780511780363.007 Published online by Cambridge University Press